Techno-Economic Sizing of Auxiliary Battery-Based Substations in DC Railway Systems

G. Graber, and A. Piccolo, *Member, IEEE*, V. Calderaro, V. Galdi
and R. Lamedica, *Senior Member, IEEE*, A. Ruvio *Student Member, IEEE*

***Abstract*—Auxiliary battery-based substations (ABSs) can enhance conventional railway feeder systems. In particular, ABSs make DC feeders located in areas far from the AC grid, able to power high-performance passenger and freight trains and store their braking energy. The paper proposes a techno-economic method to define size, position along the track, and control parameters of an ABS, with the goal to minimize the annual cost of energy (ACOE). Our approach takes into account the replacements of battery modules within the ABS expected lifetime in order to reduce costs. Numerical simulations are carried out assuming a new generation high-performance train on a real Italian 3 kV DC railway system equipped with one ABS. Although in some cases ABSs are already cheaper solutions compared to new traditional substations, the proposed sizing method allows obtaining a further reduction in the ABS cost.**

***Index Terms*—cost optimization, electric substation, energy management, energy storage system, railway system**

I. Introduction

THE current world population of 7.3 billion is expected to reach 8.5 billion by 2030, [1]. The mobility demand for people and goods is already growing in many countries and it will keep growing around the major metropolitan areas, with unsustainable environmental impacts, [1]-[2]. As confirmed by the increasing worldwide investments, rail transport is the most effective solution to meet the mobility demand because of its relatively low ratio between energy consumption and transport capacity, and its environmental advantages over other transport modes, [2].

The current technological trend ensures higher and higher transport capacity by using high-performance trains, which often move on traditional 3 kV DC lines as well as on high-voltage AC lines, limiting their power absorption, [3]-[4]. Unfortunately, timelines to upgrade existing feeder systems with more powerful conventional and/or reversible substations are much slower than the improving trend of the rolling stock performance. Moreover, the strengthening of railway feeder systems can have a heavy economic impact due to the distance from the AC transmission network, [5]-[7].

Therefore, the integration of auxiliary substations (AS) in existing DC feeder systems, equipped with energy storage systems (ESSs), can both increase the penetration of high-performance trains and reduce the upgrading operations cost because civil works for the connection to the AC transmission network are no longer necessary. In detail, ASs have to reduce excessive voltage drops on feeder systems during the trains' accelerations, and partially feed trains quite far from the traction power substation (TPS), as they approach or depart from the AS, [8]-[10]. In this way, even a one side supplied feeder system can act like a double-fed system, if one or more ASs are installed along the track. Finally, ASs can restore themselves both by storing the train's braking energy and in constant current mode through the feeder system with a very low impact in terms of voltage drops and power losses.

The most suitable ESS technologies able to meet the AS required functionalities are depicted in Fig. 1: it is clear that ASs having to partially supply a train for a short distance require battery-based ESSs. In fact, although ESS technologies such as flywheels and/or ultracapacitors are characterized by high specific power and a large number of charge/discharge cycles, they present low specific energy, [11]-[12]. Thus, they can be used in urban rail transit or metro systems mainly for voltage compensation and energy saving applications, [13]-[14]. In addition, in [15] the use of trackside flywheel-based ESSs to increase energy saving and to reduce the TPS peak load in DC metro systems is proposed, whereas [16] and [17] consider ultracapacitor-based ESSs.

Contrariwise, although last generation batteries present a lower number of charge/discharge cycles compared to other ESS technologies, they are characterized by almost the same specific power but higher specific energy, [12]. Therefore,

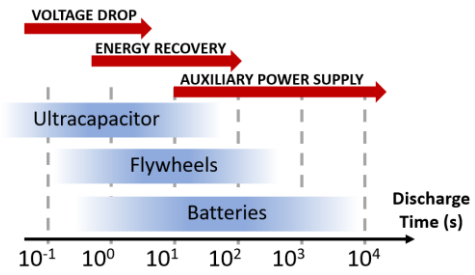

Fig. 1. ESS technologies vs. AS required functionalities.

The paper was submitted for review on December 30, 2017.

G. Graber, V. Calderaro, V. Galdi and A. Piccolo are with the Department of Industrial Engineering (DIIn), University of Salerno, Fisciano (SA), 84084 Italy (e-mail: ggraber@unisa.it, vcalderaro@unisa.it, vgaldi@unisa.it, apiccolo@unisa.it).

R. Lamedica and A. Ruvio are with the Department of Department of Astronautics Engineering, Electrical and Energy (DIAEE), University of Rome "La Sapienza", Rome (RO), 00185 Italy (e-mail: regina.lamedica@uniroma1.it, alessandro.ruvio@uniroma1.it).

auxiliary battery-based substations (ABS) represent a feasible solution able to store the required energy for partially powering trains, and to support the TPS during trains' accelerations.

The feasibility of the ABS is supported by some interesting experiences, in fact, some battery-based ESSs were recently installed in Japan and USA supporting 1.5 kV DC feeder systems, mainly to compensate voltage drops and to store trains' braking energy, [18]-[20]. In particular, [18] shows field tests performed on an ESS at Daedong substation in 2010, while the East Japan Railway Company installed a lithium-ion ESS at HAIJIMA substation on the Ome line in 2013, [19]. Test results of a Ni-MH based ESS for DC railway systems at New York City Transit in 2010, are reported in [20]. Finally, hybrid ESSs consisting of lithium-ion batteries and ultracapacitors are also proposed in [21] for high-speed railway systems. The ESSs installed in Japan and USA, during about five years of testing, have shown that voltage fluctuation is very stable (from ± 20% to ± 6% after the ESS installation at HAIJIMA substation). Moreover, the energy saving due to both voltage drop compensation and storing of the trains' braking energy is more than 20%.

The paper investigates battery technology to be integrated into ASs and concentrates the attention on techno-economic sizing and control of ESSs. A large and growing body of literature has investigated sizing procedures and control algorithm of ESSs for railway applications, [13], [16]-[25]. In particular, [13], [16] deal with joint siting and sizing of ultracapacitor-based ESSs in metro systems, whereas the preliminary sizing of battery-based ESSs in DC railway systems are proposed in [22] and [23] passing over the economic aspects of the problem. Moreover, [24] defines the specifications and design criteria of DC/DC converters for battery-based ESSs supporting railway 1.5 kV DC feeder systems, whereas a control algorithm to improve battery lifetime in power compensator for DC railway system is proposed in [25]. The paper extend the previous work [10] by presenting a new techno-economic formulation of the ABS sizing optimization problem taking into account the track topological features, the electrical characteristics of feeder system and train, and the timetable. In particular, in comparison with previous works, the main innovative contribution consists in presenting a novel method to define the ABS sizing, its position along the track and its control characteristic, with the goal to minimize the annual cost of energy (ACOE) ensuring the compliance with the safe operating constraints of the feeder system. Numerical simulations performed on a real Italian railway system show the effectiveness of the proposed ABS sizing method: in particular, the battery modules expected lifetime has grown compared to other sizing methods, further reducing costs.

II. Modelling of the Railway System

In this Section, we present a quasi-steady state model of the DC railway system including three sub-models. It describes with a good approximation power flows between feeder system, train and ABS that mainly affect economic evaluations for the ABS sizing. We also introduce the economic model, widely used in technical literature, for computing the ACOE of the feeder system equipped with ABSs. The transient analysis is postponed to the sizing procedure and it is not investigated in the paper.

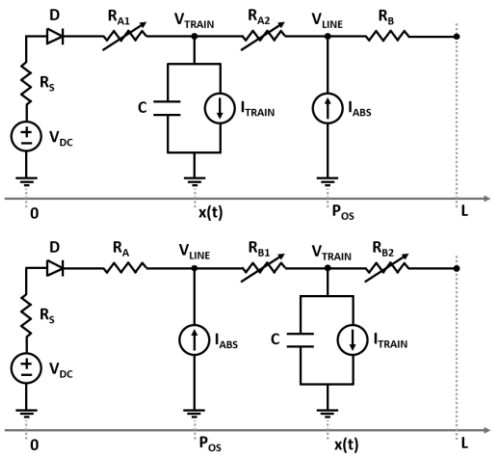

Fig. 2. Electric model of a one side supplied DC feeder system: the train before the ABS (top), and after the ABS (bottom).

A. The DC feeder system

The electric model of a one-side-supplied contact line equipped with ABSs along the track is shown in Fig. 2. The TPS, like the most of the conventional substations, is not reversible and is modelled as an ideal voltage source in series with a resistor and a diode, [3], [26]. Contrariwise, we model trains as ideal current sources: the I_{TRAIN} value is computed as the ratio of the P_{TRAIN} and the line voltage, V_{TRAIN} that changes along the track. In order to describe the receptivity of the network under regenerative braking conditions, a small capacitance in parallel to the ideal current source is added to the train model, [12], [16]. It describes the line voltage rise during the regenerative braking, which is used by the ABS controller to detect a braking train along the track. The overhead line is modelled through a set of electric resistances that change their value according to the train position. If $x(t)$ is the train position at the time t, the value of the resistances upstream R_{A1} and downstream R_{A2} of the train moving towards a generic node of the railway feeder system (TPS, ABS or another train) is calculated by:

$$\begin{cases} R_{A1}(t) = \rho \cdot x(t) \\ R_{A2}(t) = \rho \cdot [d - x(t)] \end{cases} \quad (1)$$

where ρ is the resistive coefficient, and d is the distance between two nodes that are in train upstream and downstream (according to the axis origin highlighted in Fig. 2). For systems with overhead line supply conductors and a return rail, the return resistance is lumped with the supply resistance introducing a small error (less than 3%), [14]. Since the ABS supports the feeder system during the traction phase of trains and stores their regenerative braking energy, it is represented by an ideal current source, similarly to the train model. The variation in the state of charge (SoC) according to the ABS current is calculated by using the electric models of the battery modules and the DC/DC power converter with its controller.

Finally, a nodal analysis is implemented to determine unknown voltages of the DC network, [14]. More in detail, by applying the Kirchhoff's current law, the DC feeder system is described by a set of 2*n* linear equations, where *n* are the nodes of the DC network. In particular, assuming a one-side-supplied contact line and the train before the ABS (Fig. 2 top), we can calculate the V_{TRAIN} as follows:

$$\frac{V_{DC}-V_{TRAIN}(t)}{R_S+R_{A1}}+I_{ABS}(t)=\frac{P_{TRAIN}(t)}{V_{TRAIN}(t)}+C\frac{dV_{TRAIN}}{dt} \tag{2}$$

where P_{TRAIN} is the train electric power requested/injected to the feeder system, I_{ABS} is the current supplied/absorbed by the ABS and they are both given. This is a non-linear first order differential equation. By using the finite difference method, we can rewrite (2) as:

$$\frac{V_{DC}-V_{TRAIN}(k)}{R_S+R_{A1}}+I_{ABS}(k-1)=\frac{P_{TRAIN}(k)}{V_{TRAIN}(k)}+C\frac{V_{TRAIN}(k)-V_{TRAIN}(k-1)}{\Delta T} \tag{3}$$

where $V_{TRAIN}(k)$ is the V_{TRAIN} value at time step $k\Delta T$. In each time step, we solve Eq. (3) that is a linear second order equation, reported in canonical form as follows:

$$aV_{TRAIN}^2+bV_{TRAIN}+c=0 \tag{4}$$

where:

$$\begin{aligned} a&=\left(1+\frac{C}{\Delta T}\left(R_S+R_{A1}\right)\right)\\ b&=\left(V_{DC}+\left(I_{ABS}(k-1)+\frac{C}{\Delta T}V_{TRAIN}(k-1)\right)\cdot\left(R_S+R_{A1}\right)\right)\\ c&=P_{TRAIN}(k)\cdot\left(R_S+R_{A1}\right)\end{aligned} \tag{5}$$

We select the root related to the positive sign among those of the quadratic equation according to the case $I_{ABS}(k\text{-}1)=0$, $P_{TRAIN}(k)=0$, $C=0$ where the solution have to be $V_{TRAIN}(k)=V_{DC}$. Similar results can be obtained for a train after the ABS.

B. The train

The train longitudinal dynamic is described by using the mass-point model, [3]-[4], [14], [26], according to the Newton's second law and kinematics equations (Fig. 3):

$$\begin{cases} m\dfrac{dv}{dt}=F_{mech}(t)-R_{BASE}(v)-R_{TRACK}(x)\\ x=x_0+v_0\,t+\dfrac{1}{2}\dfrac{dv}{dt}t^2\end{cases} \tag{6}$$

where v and x are the speed and position of the train respectively, and $F_{mech}(t)$ is the mechanical traction/braking force. The effective mass of the train $m = [\,(1+\varepsilon)\cdot m_T\,] + m_L$ is computed by increasing its empty mass (m_T) by a factor ε to take into account the rotating mass effect, and by adding the load mass of passengers (m_L). $R_{BASE}(v)$ is the basic resistance taking into account roll resistance and aerodynamic drag, while $R_{TRACK}(x)$ is the line resistance depending on track slopes and curves, [12]-[14], [26]. They are computed by:

$$\begin{aligned} R_{BASE}&=\alpha_1+\alpha_2|v|+\alpha_3v^2\\ R_{TRACK}&=mg\sin\left(\gamma(x)\right)+mg\frac{a}{r(x)-b}\end{aligned} \tag{7}$$

In (7), α_1, α_2 and α_3 coefficients of the Davis formula are related to the train and the track characteristics, and they can be estimated by empirical measures, or obtained by literature, [14], [26]. The curve resistance - the second term of R_{LINE} - is given by empirical formulas, as the Von Röckl's one, where

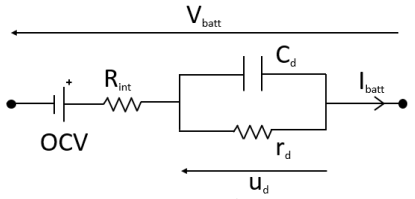

Fig. 3. First-order equivalent circuit of a battery module.

$r(x)$ is the track curvature radius, and a, b parameters depends on the track gauge [3]-[4]. Finally, $\gamma(x)$ is the slope grade of the track and g is the gravitational acceleration. Starting from an imposed speed cycle, we calculate the tractive effort at the wheels, F_{mech}. Then, going back through the efficiencies of the train components, the train electric power P_{TRAIN} is calculated as follows:

$$P_{TRAIN}=\begin{cases}\dfrac{F_{mech}\,v}{\eta_g\eta_m\eta_i}+P_{SERVICES} & F_{mech}\geq 0\\ (F_{mech}\,v)\cdot\eta_g\eta_m\eta_i+P_{SERVICES} & F_{mech}<0\end{cases} \tag{8}$$

where $P_{SERVICES}$ is the required power for auxiliary services (e.g. lighting and air conditioning), η_g represents the gear system efficiency and η_i is the average value of the inverter efficiency. In particular, η_m describes the induction motor efficiency, which is expressed in [27] as follows:

$$\eta_m=\frac{P_{out}}{P_{out}+loss}=\frac{T\omega}{T\omega+k_cT^2+k_i\omega+k_w\omega^3} \tag{9}$$

In (9), $T = F_{mech}\cdot r_{wheel} / n_{motor\_axles}$ and $\omega = v / r_{wheel}$ are the mechanical torque required by each motored axles and the angular speed, respectively, while r_{wheel} is the wheel radius and n_{motor_axles} is the number of motored axles. The $k_c\cdot T^2$ term describes the copper losses caused by the electrical resistance of the motor wires, $k_i\cdot\omega$ represents the iron losses taking into account both hysteresis and eddy current effects in the iron rotor, and $k_w\cdot\omega^3$ represents the windage losses due to friction and wind resistance of the rotor, [27]. The values of the coefficients k_c, k_i, k_w can be found through regression by using several measured values of efficiency.

C. The auxiliary battery-based substation

The first-order equivalent circuit of a lithium-ion battery module consists of four elements and is shown in Fig. 3, [28]. In particular, the ideal voltage source represents the open circuit voltage (OCV) depending on SoC value of the battery modules; the series resistor R_{int} represents the internal resistance, whereas r_d and C_d are the RC parallel circuit describing the charge transfer and the double layer capacitance, respectively.

$$\begin{aligned} &V_{BATT}(t)=OCV(t)-R_{\text{int}}I_{BATT}(t)-u_d(t)\\ &OCV(SoC)=\beta_n\cdot SoC^n+\beta_{n-1}\cdot SoC^{n-1}+\ldots+\beta_0\\ &SoC(t)=SoC(t=0)+\frac{1}{3600\cdot C_{BATT}}\int_0^t V_{BATT}(\tau)\cdot I_{BATT}(\tau)\,d\tau\\ &u_d(t)+r_dC_d\frac{du_d(t)}{dt}=r_dI_{BATT}(t)\end{aligned} \tag{10}$$

The set of equations (10) describes the electric model of the battery modules. Specifically, the first equation represents the Kirchhoff's voltage law, while the second one is the n-polynomial relationship between OCV and SoC. The third equation models the SoC update law, according to the required

current from the battery modules, and the last one is the differential equation describing the RC parallel circuit.

In (10), $u_d(t)$ is the $r_d C_d$ parallel circuit voltage, $\beta_0 \dots \beta_n$ are the interpolation coefficients and C_{BATT} is the battery module capacity. The lifetime L_R of the battery module is estimated by using the extended Peukert law taking into account the discharging current value, [32].

$$L_R = \frac{N_{LC} \cdot C_{BATT}}{\left[I_{equ} / L_R\right]^p}, \qquad I_{equ} = \sum_{j=1}^{M} I_{BATT}\left(t_j - t_{j-1}\right) \tag{11}$$

In (11), N_{LC} is the estimated number of charging/discharging cycles provided by manufacturers, $I_{BATT}(t_j)$ is the ABS current at time t_j whereas p *is* the Peukert coefficient depending on the battery technology, [12], [23]. The unknown L_R appears inside the M-term sum as well, since t_M=L_R, and thus the extended Peukert law is solved by using an iterative method such as the Levenberg-Marquardt one.

The ABS power converter is modelled by its average efficiency η describing power losses, [24]. It operates as step-up or step-down converter according to the control characteristic. In particular, given the I_{ABS} reference value provided by the ABS control characteristic, we compute the related battery current value by using (12).

$$I_{BATT} = \frac{1}{\eta} \frac{V_{LINE}}{V_{BATT}} I_{ABS} \tag{12}$$

D. The ABS control

The ABS works in four different operating modes implementing in each of them a current control according to the measured V_{LINE} and the actual SoC value, [10]. The ABS is in *discharging mode* if the line voltage is below a lower threshold value (e.g. when a train is accelerating or starting); thus, the ABS supports the DC feeder system by using the previously stored energy ($SoC > SoC^{min}$). If, instead, the line voltage exceeds an upper threshold value, (e.g. if one or more trains are braking), then the ABS stores the regenerative braking energy according to the SoC of battery modules ($SoC < SoC^{max}$), reducing the line voltage (ABS *fast charging mode*). When the ABS does not detect trains in starting or braking phase, it can also charge itself, absorbing a constant current I_{CH} from the feeder system, until it reaches a threshold value of the SoC (SoC_M), and thus the ABS is in the *slow charging mode*. The SoC_M value is computed by means of the proposed optimization algorithm described in Section III to ensure a good trade-off between the ability of the ABS to support the DC feeder system during the trains starting phase and to recover most of the braking energy. In such way, is improved the energy efficiency of the overall railway system. Finally, the ABS is in *idle mode* when it is not acting in one of the three previously described operating modes.

Fig. 4 illustrates the ABS control characteristic according to the different operating modes: it shows the ABS charging / discharging current I_{ABS} as a function of the difference (ΔV) between the rated value of V_{LINE} and its actual value, [23]. In particular, on the left side is reported the ABS control characteristic when the $SoC > SoC_M$ while the case $SoC <= SoC_M$ is reported on the right side. For both cases, in

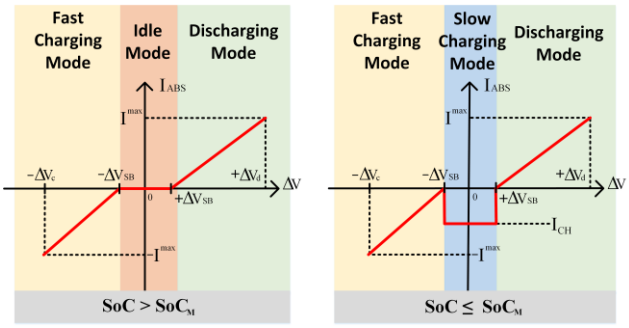

Fig. 4. ABS Control characteristics according to the SoC_M value.

the yellow area the ABS is storing the braking energy, while in the green one it supplies power to the feeder system. Finally, if $|\Delta V| < \Delta V_{SB}$ and $SoC > SoC_M$ the ABS is in the stand-by mode (red area) while in the same conditions, if $SoC <= SoC_M$ the ABS charges itself in constant current mode (blue area).

More in detail, if V_{LINE} grows due to regenerative braking ($\Delta V < 0$), the ABS is charged ($I_{ABS} < 0$), if instead V_{LINE} decreases by powering trains ($\Delta V > 0$), the ABS is discharged ($I_{ABS} > 0$). In particular, ΔV values within the [$-\Delta V_{SB}$, ΔV_{SB}] range represent a standby region where the ABS can work in idle mode or slow charging mode. When instead $|\Delta V|$ is greater than $|\Delta V_{SB}|$, the ABS is ready to supply/recover energy and is more or less responsive according to the charging/discharging slopes of the ABS control characteristic defined by the ΔV values ($-\Delta V_c$, $+\Delta V_d$) for which the ABS shows its maximum charging/discharging current, I^{max}. The relationship between I_{ABS} and ΔV is analytically expressed as follows:

$$I_{\mathrm{Re}f} = \begin{cases} I_{CH} & SoC \le SoC_M\,,\ \Delta V \in [-\Delta V_{SB}, +\Delta V_{SB}] \\ m_D \Delta V + q_D & SoC > SoC^{\min}\,,\ \Delta V \in [-\Delta V_{SB}, +\Delta V_{SB}] \\ m_C \Delta V + q_C & SoC < SoC^{\max}\,,\ \Delta V \in [-\Delta V_{SB}, +\Delta V_{SB}] \\ 0 & otherwise \end{cases} \tag{13}$$

where m_C, m_D and q_C, q_D are, respectively, the slopes and the intercepts of the charging/discharging linear relationship.

E. Economic Model

We use the annual cost of energy (ACOE) as economic metric to examine the ABS costs accounting for the time value of money, [29]. It is widely used in the technical literature and allows the railway system operator to estimate the annual cost of the feeder system and implement strategies to increase revenues. Thus, the ACOE is mathematically expressed as:

$$ACOE = CRF \cdot \left(C_I^{abs} + C_{O\&M}^{abs} + C_{REP}^{abs} + C_{O\&M}^{tps}\right) \tag{14}$$

where CRF is the capital recovery factor converting a present value into a stream of equal annual payments over a specified lifetime N, at a specified interest rate r. C_I^{abs} is the ABS capital cost, C_{REP}^{abs} is the ABS replacement cost, and $C_{O\&M}^{abs}$ and $C_{O\&M}^{tps}$ are the operation & maintenance (O&M) cost for the ABS and the TPS respectively. In particular, (15) gives the ABS capital cost according to [30]-[31]:

$$C_I^{abs} = C_P P_{ABS} + C_E E_{ABS} + C_{FC} \tag{15}$$

where C_P and C_E are the ABS specific costs, whereas C_{FC} are the ABS fixed costs. In (16), O&M cost is defined as:

$$C_{O\&M} = \sum_{n=1}^{N} \frac{C_n}{(1+r)^n} \tag{16}$$

where C_n is the annual operations cost of year n including both fixed (C_f) and variable (C_v) costs. In (17) we expressed C_n for the ABS and the TPS by using the *abs* and *tps* subscripts, respectively, [29]-[31].

$$\begin{aligned} C_n^{abs} &= C_f^{abs} P_{ABS} + C_v^{abs} N_d E_d^{abs} + \frac{E_d^{abs}}{\eta_{CH}} C_{CH} \\ C_n^{tps} &= C_f^{tps} P_{TPS} + C_v^{tps} N_d E_d^{tps} \end{aligned} \tag{17}$$

In (17), E_d^{abs} and E_d^{tps} are the energy supplied by the ABS and the TPS in a day, respectively, P_{TPS} is the TPS rated power, and N_d is the number of days in which the feeder system is active within one year. Moreover, the cost for charging the ABS during the night is given by the product of E_d^{abs} and the electricity cost coefficient C_{CH} divided by the average value of the charging efficiency η_{CH}. The replacement cost of battery modules within the ABS lifetime is also added to the ABS total cost, [30]-[31], and it is expressed in (18):

$$C_{REP}^{abs} = C_{RP}[(1+r)^{-L_R} + (1+r)^{-2L_R} + \ldots] \tag{18}$$

where C_{RP} is the future value of replacement cost and L_R is the battery replacement period estimated by using the extended Peukert law. ABS cost and Peukert coefficients are listed in Table I for different battery technologies, [11].

TABLE I
ABS COST AND PEUKERT COEFFICIENTS

Parameters	Technologies			Unit
	Li-ion	NaS	VRB	
C_P	120	350	370	€/kW
C_E	440	400	550	€/kWh
C_f	7.2	9.6	11.3	€/kW
C_v	0.0011	0.003	0.0038	€/kWh
η_{CH}	0.90	0.80	0.75	%
Lifetime (DoD=100%)	6000	4000	8000	#cycles
p	1.17	1.28	1.23	-

III. THE ABS SIZING PROBLEM

The problem we aim to solve consists in finding the ABS rated power and energy, position and control parameters able to minimize the sum of ABS and TPS costs. We also take into account the topological characteristics of the track, the electrical ones of the feeder system, the vehicle mechanical features and its timetable.

A. Mathematical formulation

We consider as objective function the ACOE of the DC feeder system equipped with one ABS. The decision variable is the set $\bar{x}_c$ consisting in the rated value of the ABS power and capacity, the ABS position along the track and the ABS control parameters.

$$\bar{x}_c = \{P_{ABS}, E_{ABS}, P_{os}, \Delta V_{SB}, \Delta V_c\, \Delta V_d, I_{CH}, SOC_M\} \tag{19}$$

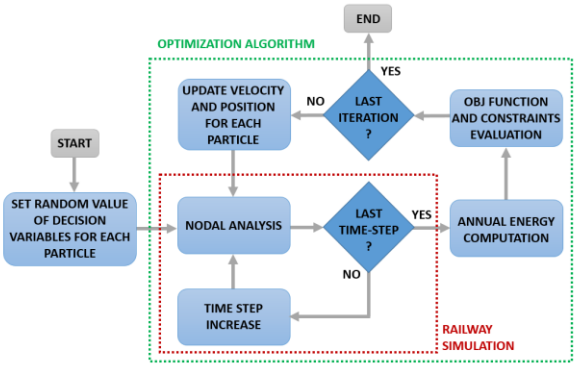

Fig. 5. Flow chart of the PSO-based solution algorithm.

Thus, the optimization problem is formulated as follows:

$$\begin{aligned} Z: \min_{\bar{x}_c} \quad & ACOE(\bar{x}_c) \\ s.t. \quad & P_{ABS}^{\min} \le P_{ABS} \le P_{ABS}^{\max} \\ & E_{ABS}^{\min} \le E_{ABS} \le E_{ABS}^{\max} \\ & 0 \le P_{os} \le L^{\max} \\ & +\Delta V_{SB} \le \Delta V_D \le V_{LINE}^{\min} \\ & V_{LINE}^{\max} \le -\Delta V_C \le -\Delta V_{SB} \\ & 0 \le I_{CH} \le I_{CH}^{\max} \\ & \Delta V_{SB}^{\min} \le \Delta V_{SB} \le \Delta V_{SB}^{\max} \\ & SoC_M^{\min} \le SoC_M \le SoC_M^{\max} \\ & V_{LINE}^{\min} \le V_{LINE}(t) \le V_{LINE}^{\max} \quad \forall t \le T \\ & 0 \le P_{TPS}(t) \le P_{TPS}^{\max} \quad \forall t \le T \\ & I_{BATT}^{\min} \le I_{BATT}(t) \le I_{BATT}^{\max} \quad \forall t \le T \\ & V_{BATT}^{\min} \le V_{BATT}(t) \le V_{BATT}^{\max} \quad \forall t \le T \\ & SoC^{\min} \le SoC(t) \le SoC^{\max} \quad \forall t \le T \end{aligned} \tag{20}$$

where L^{max} is the track length, $V_{LINE}^{\min}$ and $V_{LINE}^{\max}$ are the minimum and maximum allowable line voltage values according to the standard BS EN 50163 and IEC 60850 (-33% and +20% of the V_{LINE} rated value, respectively). Moreover, T is the total simulation time, P_{TPS} is the power supplied by the main substation, and V_{batt}, I_{batt} and SoC are the current, voltage and state of charge related to the ABS battery modules, respectively: each of them is limited to their minimum and maximum value. Although ABS position and control parameters do not directly affect the ABS total cost, they can make a given sizing solution (P_{ABS} and E_{ABS}) feasible or unfeasible in terms of safe operating conditions of the feeder system. However, the relationship between the ABS sizing (rated power and capacity), its position along the track and its control parameters is not a closed-form expression. Thus, we solve it by using a railway system simulator, which is able to verify the safe operating conditions of the DC feeder system, starting from a given value of the ABS sizing, position and set of control parameters.

B. Solution algorithm

The proposed sizing problem is a non-linear optimization problem with real decision variables and linear constraints. However, since the battery modules are commercially available only in discrete sizes and the ABS can be installed only in a few positions along the track, we solve the sizing problem assuming discrete decision variables. Thus, it is

possible to solve an intractable problem, such as the proposed one presenting no closed-form expressions, through to a brute force search. To improve its performances in terms of computing time without straining the goodness of the solution, we use the particle swarm optimization (PSO) to explore more quickly the solution space, [33]. The brute force search will be used to validate the heuristic approach.

Fig. 5 shows the flow chart of the solution algorithm. After initializing the set $\bar{x}_c$ of each particle with a random value (a sizing solution for the ABS), the algorithm performs the nodal analysis by using the railway simulator. In each simulation we assume in t=0: V_{TRAIN} equal to the rated value of V_{LINE}, and P_{TRAIN}=I_{ABS}=0. Then, the ACOE and the constraints compliance are evaluated for each particle. Finally, the position and the velocity of each particle are updated and the algorithm repeats again these steps until convergence.

IV. Numerical Simulation

The effectiveness of the proposed ABS sizing method is verified on the Italian railway line linking *Roma Termini* rail station to the *international airport Leonardo da Vinci* in Rome. The railway system simulator is coded in Matlab™.

A. Case study

Our analysis is performed on the route section *Magliana-Fiumicino* of the track *Roma Termini-Fiumicino*. At present, a direct train (peak power 2800 kW) leaves from *Roma Termini* station every 30 minutes, and a high-traffic train (peak power 3500 kW) leaves from *Roma Tiburtina* station every 15 minutes. The DC feeder system is a 3 kV DC one-side-supplied overhead line consisting in one conventional (not reversible) electric substation, located in *Magliana*, and an ABS, assumed by the authors, located in *Fiumicino*. Since high-performance trains can provide a single journey over multiple electrification systems without interruption, the proposed ABS can be an interesting solution to enhance the 3 kV DC feeder system supplying the line *Roma Termini* rail station–*Fiumicino* rail station (inside the *International Airport Leonardo da Vinci*). In such way, high-performance trains reaching *Roma Termini* are able to continue until *Fiumicino* improving the existing service.

Several simulations are carried out in which one high-performance train having similar characteristics to the ETR 1000 model of Ferrovie dello Stato Italiane Group, moves in the two opposite directions following the same speed cycle. We assume the train leaving every 60 minutes from the *Roma Termini* rail station, 15 hours in one day and 300 days in one year. The speed cycle and the track altimetry are shown in Fig. 6. The maximum speed reached by the train due to track limitations is highlighted in dotted black line. DC feeder system, train, and ABS are characterized by parameters listed in Table II, [4], [27]-[28]. In the following, we compare the performance of two different ABS sizing methods: the proposed optimal sizing (ACOE_size) and a typical battery-sizing method aimed to reduce as much as possible the rated power and capacity of the ABS (MIN_size) according to the safe operating constraints of the feeder system, such as [20]. Moreover, we compare the performance of the brute force search and the PSO as solution algorithms.

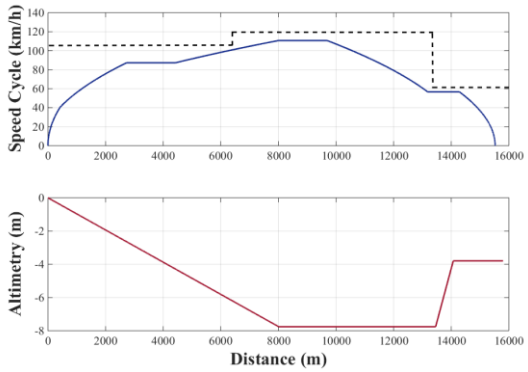

Fig. 6. Speed cycle and track altimetry (MAGLIANA-FIUMICINO).

TABLE II
Railway System Parameters

Parameter	Value	
TRACK		
Length	15.8	km
Davis formula coef. α_1	1.2	N / kN
Davis formula coef. α_2	$1.6 \cdot 10^{-3}$	N / (kN · km/h)
Davis formula coef. α_3	$15 \cdot 10^{-4}$	N / (kN · km/h)^2
Von Röckl formula coef. *a*	0.65	m
Von Röckl formula coef. *b*	55	m
DC FEEDER SYSTEM		
Rail electric resistance	0.062	Ω/km
Substation maximum power	5400	kW
Substation DC voltage	3000	V
Substation internal resistance	0.013	Ω
TRAIN		
Loaded weight	500	t
Maximum Acceleration	0.7	m/s^2
Maximum traction power	9800	kW
Auxiliaries power	300	kW
Auxiliaries use coef.	0.75	-
Wheel diameter	1040	mm
Number of motored axles	8	-
Gear-box efficiency	0.98	-
Inverter average efficiency	0.9	-
Copper loss coef. k_c	0.3	Nm^{-2}
Iron loss coef. k_i	0.01	s·rad^{-1}
Windage loss coef. k_w	$5.0 \cdot 10^{-6}$	s·rad^{-3}
ABS		
Battery technology	Li-ion	-
Rated voltage	2000	V
Maximum current	3	C
Max. (Min.) SoC value	95 (30)	%
Cell nominal OCV	3.2	V
Cell internal resistance	0.001	Ω
Cell double layer resistance	0.003	Ω
Cell double layer capacitance	3000	F

B. Results and discussion

The actual operating conditions of the line *Magliana-Fiumicino* are described in [34]. The simulation results show that only one high-performance train dramatically reduces the average useful voltage on the feeder system. In particular, whithout considering the existing service, the line voltage could reach almost 1900 V during the traction phase, not allowing safe operating conditions. Moreover, without

assuming an ABS or a new TPS, the existing DC feeder system is not able to move a high-performance train on the opposite direction. Preliminary results show that at least a new 3 MW TPS located at *Fiumicino* rail station would be necessary. Although 3 MW is not a standard TPS size used by Italian national railways and the best practices for planning suggest to oversize new TPSs to take into account future and/or more severe operating conditions, however we use this reference value to perform comparative evaluations with the ABS, [5]. In the following, we estimate the net present value of a conventional TPS highlighting four key contributions according to the cost estimation reported in [6].

Rectifier set: ex-works cost (i.e. without transport, insurance and customs costs between seller and buyer) of a 3 MW rectifier set consisting of transformer, rectifier, and ancillaries, varies from 1100 k€ to 1400 k€.

Operation & Maintenance: O&M cost for a new TPS including electricity cost, service cost and maintenance cost, can be estimated according to the economic considerations introduced in Section IV.

Civil works: this cost varies from 150 k€ (assuming no need for significant earthworks, etc.), to 290 k€ (if the ground requires piling, structural works, etc.).

Connection to AC grid: according to TERNA data (the Italian TSO), the closest connection point to the AC grid is located about 40 km from *Fiumicino* rail station. Thus, a target cost of 800 k€ has been reasonably considered for our cost estimation.

The connection to the AC grid represents about 26% of the new TPS total cost, making it not very attractive from the economic point of view. Contrariwise, the ABS is a cheaper solution: Table III shows the comparison in terms of battery technologies by using the two sizing methods. Although lithium-ion batteries are characterized by lower charging / discharging cycles than vanadium redox batteries (VRB) and lower energy density than sodium sulphur (NaS) batteries, their widespread market penetration and technological maturity make them a cheaper solution compared to other battery types, [12], [35]. Although lead-acid batteries are the oldest technology and have the lowest cost per Wh and kW, we have not considered lead-acid batteries in our analysis because they are characterized by limited number of charging / discharging cycles, low charging current due to sulfation, limited calendar life, environmental concerns, and lower efficiency, [34]. Thus, we assume in the following a lithium-ion ABS because it represents in our analysis the best compromise between cost and modules replacements. We compared the results obtained by using the proposed PSO-based solution algorithm to those of the brute force search. It is worth noting that by imposing 20,000 iterations and 25 particles, the goodness of the solution is not affected but the computing time is reduced by about 40%. Moreover, Table IV summarizes the cost comparison between a new TPS and a lithium-ion ABS. Obtained results show that the net present value of a 3 MW new TPS is at least 12.9% higher than that of an ABS and its ACOE is 9.6% higher. Although the MIN_size method leads to a smaller ABS, its ACOE is the 11.1% greater than that obtained by using the ACOE_size procedure. In fact, the MIN_size method forces the ABS to more stressful

TABLE III
COMPARISON ON BATTERY MODULES TECHNOLOGY

	Modules replacement			ABS ACOE [k€/year]		
	Li-ion	NaS	VRB	Li-ion	NaS	VRB
ACOE_size	1	2	1	176	215	231
MIN_size	2	3	1	201	227	254

TABLE IV
TPS VS. ABS COST COMPARISON

Parameter	TPS	ABS (MIN_size)	ABS (ACOE_size)	Unit
Position	15.8	15.8	15.8	km
Rated capacity	-	1000	1200	kWh
Rated power	3000	2800	3000	kW
Replacement period	-	8	10	year
Expected lifetime	20	20	20	year
Interest rate	4	6	6	%
Net present value	3120	2688	2433	k€
ACOE	228	201	176	k€/year

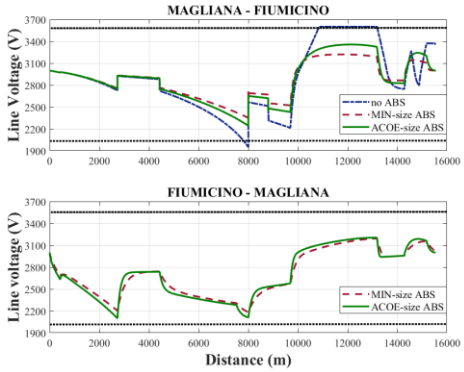

Fig. 7. Comparison on line voltage trend.

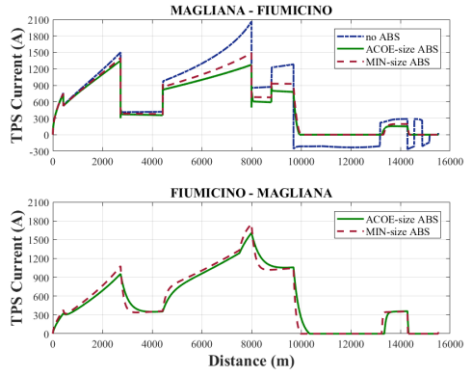

Fig. 8. Comparison on TPS current trend.

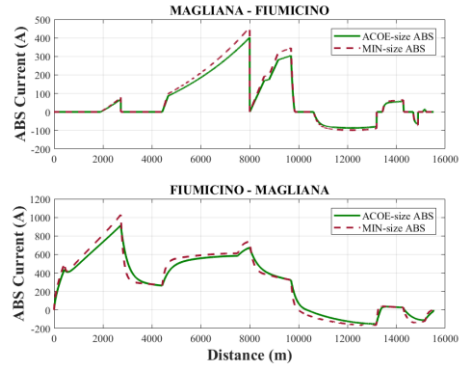

Fig. 9. Comparison on ABS current.

TABLE V
COMPARISON ON ABS CONTROL PARAMETERS

	ΔV_{SB} [V]	SoC_{LIM} [%]	I_{CH} [A]	ΔV_d [V]	ΔV_c [V]
ACOE_size	100	70	50	420	485
MIN_size	80	60	65	310	390

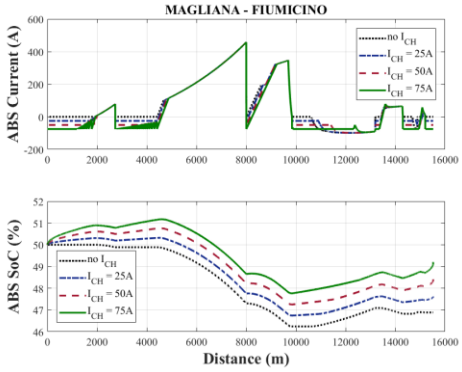

Fig. 10. Effect of the constant charging current: ABS current and SoC trends on the line MAGLIANA-FIUMICINO.

operating conditions and thus it makes necessary replace more times the battery modules during the ABS expected lifetime.

In detail, Fig. 7 shows the line voltage trends with the MIN_size and ACOE_size ABS comparing them with the line voltage trend without ABS. On the line *Magliana-Fiumicino*, both the ABS sizing methods allow obtaining limited line voltage variations avoiding the braking chopper use due to over voltages. The MIN_size ABS leads to a lower reduction in voltage drop (about 20%) and power losses (5.17%) although its sizing is slightly smaller. However, the ABS sized for the line *Magliana-Fiumicino* is not able to support the feeder system when a high-performance train moves in the opposite direction. Obtained results show that it is necessary an ABS power rating at least twice to keep the line voltage variation within the allowed limits on the line *Fiumicino-Magliana*. In particular, the MIN_size method compared with the ACOE_size, presents a slighty better reduction in voltage drops (26.67%) and power losses (3.14%). Fig. 8 shows the TPS current trend on the line *Magliana-Fiumicino* comparing the two sizing methods. Without ABS, the TPS current trend matches the train current trend, while a slightly reduction in the train peak current due to reduced voltage drops is obtained by using the ABS. Indeed, the MIN_size ABS supplying about 482 A reduces the TPS peak current by about 37.5%, while the ACOE_size ABS allows obtaining a reduction of about 30%. The ABS, on the line *Fiumicino-Magliana* supplies a peak current of about 1042 A and 921 A by using the MIN_size and ACOE_size, respectively. The TPS peak currents are about 1590 A and 1780 A, respectively.

The trends of the ABS delivered/absorbed current are shown in Fig. 9 by using ACOE_size and MIN_size methods. In particular, on the line *Magliana-Fiumicino* the ABS slightly contributes to power the train during its starting phase while the ABS supplied current increase as the train is approaching. A train moving on the line *Fiumicino-Magliana*, instead, is supplied by the ABS not only during the its starting phase but also while the train moves away reducing the TPS load of about 600 A and therefore power losses (the ABS supplied current is lower than 100 A after 10km). Although the two methods lead to same results regarding the ABS positioning, they significantly differ in the value of the ABS control parameters. Table V summarizes the comparison between the MIN_size and ACOE_size methods: the first one allows obtaining a smaller ABS characterized by largest operating characteristic slope (about 24.2%) with respect to the proposed method. The join effect of a smaller sizing and more responsive control brings the ABS to more stressful operating conditions reducing the lifetime of its battery modules.

Finally, Fig. 10 depicts the ABS current and SoC trends on the line *Magliana-Fiumicino* by imposing different I_{CH} values in the ACOE_size method. The ABS current trend with constant charging current only differs in time intervals in which the line voltage is within the standby zone and it shows a constant absorption from the feeder system. By increasing the I_{CH} value from 25 A to 75 A, the effect on the line voltage is negligible, whereas the SoC value at the end of the trip is also increased from 1% to 3% compared to the case with no I_{CH} current. It is worth to note that power losses on the line also increase from 0.36% to 1.45%.

V. CONCLUSION

In the paper, we proposed a novel sizing method for ABS, able to minimize the ACOE of the railway feeder system according to its safe operating constraints. In particular, the railway system is modelled and a simulation tool to quantify the power flow on the DC feeder system is implemented. The effectiveness of the proposed sizing method is verified in simulation on a real Italian DC railway system equipped with a Lithium-ion ABS, and in which moves a high-performance train such as the ETR 1000 model.

Obtained results showed that the ABS is more attractive from the economic point of view than a new TPS requiring high cost for connecting it to the AC grid. In particular, the proposed sizing method allows further reducing (about 13%) the ACOE of the railway system respect to a method minimizing the ABS overall sizing. Finally, our approach taking also into account the ABS control, allows extending the battery modules lifetime, reducing their replacements during the ABS expected lifetime and then reducing costs.

REFERENCES

[1] International Energy Agency (IEA), "World Energy Outlook," 2015, *available on line at url: http://www.worldenergyoutlook.org/weo2015/*

[2] International Energy Agency (IEA), "Railway Handbook," 2015, *available on line at url: http://www.uic.org/IMG/pdf/iea-uic_2015-2.pdf*

[3] C. N. Pyrgidis, "Railway Transportation Systems: Design, Construction and Operation," 2016, *CRC Press.*

[4] F. Perticaroli, "Sistemi elettrici per i trasporti," 2nd Edition, 2001, *CEA.*

[5] L. Abrahamsson, L. Soder, "Railway Power Supply Investment Decisions Considering the Voltage Drops - Assuming the Future Traffic to Be Known," in *Proc.* ISAP, 2009, pp. 1-6.

[6] P. Keen, R. Phillpotts, "Low Cost Electrification for Branch Lines," DeltaRail, Derby, UK Tech. Rep. ES-2010-003, July 2010.

[7] V. Gelman, "Energy Storage That May Be Too Good to Be True," *IEEE Vehicular Technology Magazine*, Dec. 2013, pp. 70-80.

[8] T. Konishi, M. Tobita, "Fixed Energy Storage Technology Applied for DC Electrified Railway (Traction Power Substation)," in *Proc. ESARS*, 2012, pp. 1-6.

[9] M. Sadakiyo, N. Nagaoka, A. Ametani, S. Umeda, Y. Nakamura, J. Ishii, "An optimal operating point control of lithium-ion battery in a power compensator for DC railway system," in *Proc. UPEC*, 2007, pp. 681-686.

[10] V. Calderaro, V. Galdi, G. Graber, A. Capasso, R. Lamedica, A. Ruvio, "Energy Management of Auxiliary Battery Substation Supporting High-Speed Train on 3 kV DC Systems," in *Proc. ICRERA*, 2015, pp. 1-6.

[11] H. Chen, T.N. Cong, W. Yang, C. Tan Y.Li, Y. Ding, "Progress in electrical energy storage system: A critial review," *Progress in Natural Science*, Vol.19, No.3, March 2009, pp. 291-312.

[12] M. Farhadi, O. Mohammed, "Energy Storage Technologies for High-Power Applications," *in IEEE Trans. on Industry Applications*, Vol. 52, No. 3, May-June 2016, pp. 1953-1961.

[13] V. Calderaro, V. Galdi, G. Graber, A. Piccolo, "Optimal Siting and Sizing of Stationary Supercapacitors in a Metro Network using PSO," in *Proc. ICIT*, 2015, pp. 1-6.

[14] A. Capasso, R. Lamedica, A. Ruvio, M. Ceraolo, G. Lutzemberger, "Modelling and simulation of electric urban transportation systems with energy storage", in *Proc. EEEIC*, 2016, pp. 1-5.

[15] A. M. Gee, R.W. Dunn "Analysis of Trackside Flywheel Energy Storage in Light Rail Systems," *IEEE Trans. on Vehicular Technology*, Vol. 64, No. 9 Sept. 2015, pp. 3858-3869.

[16] T. Ratniyomchai, S. Hillmansen, P. Tricoli, "Optimal Capacity and Positioning of Stationary Supercapacitors for Light Rail Vehicle systems," in *Proc. SPEEDAM*, 2014, pp. 807-812.

[17] R. Barrero, X. Tackoen, and J. Van Mierlo, "Quasi static simulation method for evaluation of energy consumption in hybrid light rail vehicles," in *Proc. VPPC*, 2008, pp. 1-7.

[18] Lee Hanmin , Kim Gildong, Lee Changmu, Joung Euijin "Field Tests of DC 1500 V Stationary Energy Storage System," *Int. Journal of Railway*, Vol. 5, No. 3, Sep. 2012, pp. 124-128.

[19] H. Hayashiya, D. Hara, M. Tojo, K. Watanabe, M. Hino, T. Suzuki, H. Okamoto, H. Takahashi, T. Kato, M. Teshima "Lithium-ion battery installation in traction power supply system for regenerative energy utilization," in *Proc. PEMC*, 2014, pp. 119-124.

[20] K. Ogura, K. Nishimura, T. Matsumura, C. Tonda, E. Yoshiyama, M. Andriani, W. Francis, R.A. Schmitt, A. Visgotis, N. Gianfrancesco, "Test Results of a High Capacity Wayside Energy Storage System Using Ni-MH Batteries for DC Electric Railway at New York City Transit," in *Proc. IEEE-Green*, 2011, pp. 1-6.

[21] S. de la Torre, A. J. Sánchez-Racero, J. A. Aguado, M. Reyes, O. Martínez, "Optimal Sizing of Energy Storage for Regenerative Braking in Electric Railway Systems," *in IEEE Trans. on Power Systems*, Vol. 30, No. 3, May 2015, pp. 1492-1500.

[22] M. Conte, F. Vellucci, M. Pasquali, "Design Procedures of Lithium-ion Battery Systems: the Application to a Cable Railway," in *Proc. ICCEP*, 2011, pp. 257-264.

[23] T. Iwase, J. Kawamura, K. Tokai, M. Kageyama, "Development of battery system for railway vehicle," in *Proc. ESARS*, 2015, pp. 1-6.

[24] Zhaofeng Li, Shunichiro Hoshina, Nobuhiko Satake, Masayuki Nogi, "Development of DC/DC Converter for Battery Energy Storage Supporting Railway DC Feeder Systems," *in IEEE Trans. on Industry Applications*, Vol. 52, No. 5, Sept-Oct. 2016, pp. 4218-4224.

[25] T. Niwa, N. Nagaoka, N. Mori, A. Ametani, S. Umeda, "A control method of charging and discharging lithium-ion battery to prolong its lifetime in power compensator for DC railway system," in *Proc. UPEC*, 2008, pp. 1-5.

[26] M. Z.Chymera, A. C. Renfrew, M. Barnes J. Holden, "Modeling Electrified Transit Systems," *in IEEE Trans. On Vehicular Technology*, Vol. 59, No. 6 July 2010, pp. 2748-2756.

[27] A. Mahmoudi, Wen L. Soong, G. Pellegrino, E. Armando, "Efficiency maps of electrical machines," in *Proc. ECCE*, 2015, pp. 2791-2799.

[28] Yao-Ching Hsieh, Tin-Da Lin, Ruei-Ji Chen, Hong-Yu Lin, "Electric circuit modelling for lithium-ion batteries by intermittent discharging," *IET Power Electronics*, Vol. 7, No. 10, Oct. 2014, pp. 2672 - 2677.

[29] M. H. El-Far, W. G. Morsi, "Cost-Effectiveness Analysis of Battery Energy Storage in Distribution Systems Embedded with Plug-in Electric Vehicles," in *Proc. CCECE*, 2015 pp.51-56.

[30] F. A. Chacra, P. Bastard, G. Fleury, R. Clavreul, "Impact of energy storage costs on economical performance in a distribution substation," *IEEE Trans. on Power Systems*, Vol. 20, No. 2, may 2005, pp. 684-691.

[31] P. Poonpun, Ward T. Jewell, "Analysis of the Cost per Kilowatt Hour to store Electricity," *IEEE Trans. on Energy Conversion*, Vol. 23, No. 2, June 2008, pp. 529-534.

[32] D. Liu, Wei Xie, H. Liao, Yu Peng, "An Integrated Probabilistic Approach to Lithium-Ion Battery Remaining Useful Life Estimation," *IEEE Trans. on Instrumentation and Measurement*, Vol. 64, No. 3, March 2014, pp. 660-670.

[33] Y. del Valle, G.K. Venayagamoorthy, S. Mohagheghi, J.-C. Hernandez, R.G. Harley, "Particle Swarm Optimization: Basic Concepts, Variants and Applications in Power Systems," *IEEE Trans. on Evolutionary Computation*, March 2008, Vol. 12, pp. 171-195.

[34] A. Capasso, M.C. Falvo, U. Grasselli, R. Lamedica, R. Bartoni, M. Francisi, G. Maranzano, "A plannyng study on power systems of metro-transit transportation system," in *Proc. SPEEDAM*, 2008, pp. 1027-1032

[35] International Energy Agency (IEA), "Technology Road map - Energy storage," 2014, *available on-line at url*: https://www.iea.org/publications /freepublications/publication/TechnologyRoadmapEnergystorage.pdf

Giuseppe Graber (M'14) received the M.Sc. degree in Electronic Engineering and the Ph.D. in Information Engineering from the University of Salerno, Italy, in 2011 and 2016, respectively. Currently, he is research fellow and collaborates with the Department of Industrial Engineering, in the same University. His main research interests focus on innovative solutions for increasing energy efficiency in railway systems and impact assessment of electric vehicles charging demand in smart grids.

Vito Calderaro (SM'16) received the M.Sc. degree in Electronic Engineering and the Ph.D. degree in Information Engineering from the University of Salerno, Italy, in 2001 and 2006, respectively. He is a Research Fellow with the Department of Industrial Engineering. His current research focuses on integration of distributed generation and storage systems on electrical distribution networks, soft computing methodologies in power system applications, and protection and diagnosis of complex systems.

Vincenzo Galdi (SM'17) received the M.Sc. degree summa cum laude in Electronic Engineering from the University of Salerno, Italy, in 1994, and the Ph.D. degree in Electrical Engineering from the University of Napoli, Italy, in 1999. Since 2003, he is an Associate Professor at the University of Salerno. His current research interests include application of ICT to power systems, to power management and energy efficiency in transportation systems, smart grids and ITS.

Antonio Piccolo (M'06) received the M.Sc. degree in Electrical Engineering from the University of Napoli, Italy, in 1974. Since 1990, he is a Full Professor with the Department of Industrial Engineering, University of Salerno, Italy. He has authored more than 130 papers mainly in international journals and conferences in the fields of power systems, where He served as reviewer and session chair. His main fields of interest are the application of ICT to electric energy infrastructures and transportation systems.

Regina Lamedica (SM'16) .

Alessandro Ruvio (M'17) received the M.Sc. with honors in Electrical Engineering from the University of Rome "La Sapienza", Italy, in 2012. Since 2013, he is with Dept. of Electrical Engineering as Assistant Research. Currently, he is a Ph.D. Student. His main research interests include power system analysis and computer applications to electrified transport systems. In April 2013, he has been awarded with the title "Excellent Graduate" for the year 2011-2012.